

Atom-membrane cooling and entanglement using cavity electromagnetically induced transparency

Claudiu Genes,¹ Helmut Ritsch,¹ Michael Drewsen,² and Aurélien Dantan²

¹*Institute for Theoretical Physics, University of Innsbruck, Technikerstrasse 25, A-6020 Innsbruck, Austria*

²*QUANTOP, Danish National Research Foundation Center for Quantum Optics, Department of Physics and Astronomy, University of Aarhus, DK-8000 Aarhus C, Denmark*

(Received 2 May 2011; published 14 November 2011)

We investigate a hybrid optomechanical system composed of a micromechanical oscillator as a movable membrane and an atomic three-level ensemble within an optical cavity. We show that a suitably tailored cavity field response via electromagnetically induced transparency (EIT) in the atomic medium allows for strong coupling of the membrane's mechanical oscillations to the collective atomic ground-state spin. This facilitates ground-state cooling of the membrane motion, quantum state mapping, and robust atom-membrane entanglement even for cavity widths larger than the mechanical resonance frequency.

DOI: [10.1103/PhysRevA.84.051801](https://doi.org/10.1103/PhysRevA.84.051801)

PACS number(s): 42.50.Gy, 03.67.Bg, 42.50.Lc, 85.85.+j

Recent years have witnessed tremendous progress toward the control of mechanical motion at the quantum limit in micro- and nano-optomechanical systems [1]. While cavity optomechanical phenomena are traditionally investigated with solid-state optomechanical systems—micromirrors, cantilever tips, toroidal resonators, movable membranes, etc.—cold atomic gasses placed in high-finesse optical cavities [2] have also been successfully used to implement equivalent Hamiltonians at ultralow temperatures. Consequently, several proposals have suggested a combination of both approaches to realize hybrid optomechanical systems [3–5], in which well-controlled atomic systems can be interfaced with solid-state mechanical resonators. These can benefit from the well-established atomic physics methods for cooling, trapping, state preparation, control, and readout and can properly tailor the atom-cavity response function.

We propose here a hybrid system composed of a mechanical oscillator, in the form of a movable membrane, and a three-level atomic medium operated in an electromagnetically induced transparency (EIT) configuration within the optical cavity [6,7]. We show how the cavity field response can be tailored [4,8] by the EIT interaction in order to strongly couple the membrane motion to the collective atomic ground-state spin. The sharp and tunable nature of the cavity field EIT resonance efficiently addresses either the Stokes or anti-Stokes motional sidebands of the membrane (which is reminiscent of EIT cooling of ions [9]), even in the bad-cavity limit, that is, when its mechanical resonance frequency is much smaller than the cavity linewidth. We show in particular how to engineer beamsplitter- or down-conversion-type Hamiltonians [10] between the membrane motion and the collective atomic spin, which can be exploited for efficient optomechanical cooling, quantum state mapping, or robust atom-membrane entanglement generation. Such interactions would be especially appealing for low mechanical resonance frequency (sub-megahertz) mechanical oscillators [11], coupled to cold atoms or Bose-Einstein condensates [2,5,12] or ion crystals [13] in low-finesse optical cavities.

Model. Let us consider an ensemble of N three-level atoms or ions in a Λ configuration coupled to a control laser and a cavity field mode on the two upward transitions. The level frequency separations are ω_{13} , ω_{23} as optical transitions and

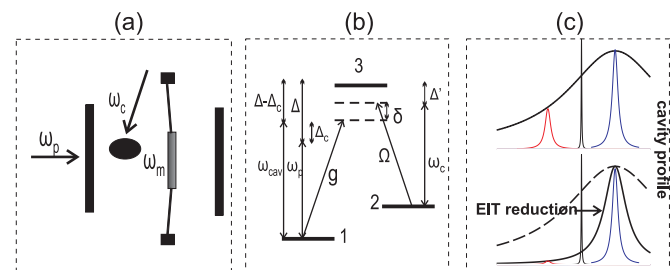


FIG. 1. (Color online) (a) Hybrid optomechanical system composed of an atomic ensemble and a mechanical oscillator enclosed in an optical cavity. (c) Cavity field transmission frequency profile for (un)resolved sideband cooling of the membrane motion in the bad cavity limit (upper) and cavity EIT-resolved sideband cooling (lower).

ω_{12} in the microwave domain. The cavity field a is driven at ω_p , close to a cavity resonance ω_{cav} . A single membrane vibrational mode at frequency ω_m is considered with corresponding ladder operators b, b^\dagger . In terms of the atomic operators $\sigma_{\alpha\beta}^{(j)}$ ($j = 1 - N$), the free Hamiltonian is (with $\hbar = 1$) $\mathcal{H}_0 = \omega_{21} \sum_j \sigma_{22}^{(j)} + \omega_{31} \sum_j \sigma_{33}^{(j)} + \omega_{cav} a^\dagger a + \omega_m b^\dagger b$. With an extra control laser driving on the 2–3 transition at frequency ω_c , the atom-field interaction is $\mathcal{H}_{at-f} = -g(\sum_j \sigma_{31}^{(j)} a + \text{H.c.}) - \Omega(\sum_j \sigma_{32}^{(j)} e^{-i\omega_c t} + \text{H.c.})$, where g is the single atom-cavity field coupling strength and Ω is the control field Rabi frequency. In the case of an inhomogeneous coupling distribution, N represents the effective number of atoms interacting with the cavity field [13]. The optomechanical interaction, proportional to the cavity resonance shift due to the displacement of the membrane, is $\mathcal{H}_{f-m} = -G_0 a^\dagger a (b^\dagger + b)$, where G_0 is the bare optomechanical coupling [11,15].

We consider a typical EIT regime for which the cavity field is much weaker than the control field ($g \langle a \rangle \ll \Omega$), and most of the atoms are in level 1. This allows us to make the standard bosonization approximation and map the spin algebra to a harmonic oscillator algebra via the transformation $1/\sqrt{N} \sum_j \sigma_{12,13}^{(j)} \rightarrow c_{2,3}$ with $[c_{2,3}, c_{2,3}^\dagger] = 1$. In a rotating frame that redefines dynamics in terms of detunings, $\Delta_{cav} = \omega_{cav} - \omega_p$, $\Delta = \omega_{31} - \omega_p$, $\Delta' = \omega_{32} - \omega_c$, and $\delta = \Delta - \Delta'$,

one can derive the following set of coupled equations of motion that will be the starting point of our calculations:

$$\dot{c}_3 = -(\gamma + i\Delta)c_3 + ig_N a + i\Omega c_2 + c_3^{in}, \quad (1a)$$

$$\dot{c}_2 = -(\gamma_c + i\delta)c_2 + i\Omega c_3 + c_2^{in}, \quad (1b)$$

$$\dot{a} = -(\kappa + i\Delta_{\text{cav}})a + ig_N c_3 + iG_0 a(b^\dagger + b) + a_{in}, \quad (1c)$$

$$\dot{b} = -(\gamma_m/2 + i\omega_m)b + \gamma_m/2b^\dagger + iG_0 a^\dagger a + b_{in}, \quad (1d)$$

where κ , γ_m , γ , and γ_c are the decay rates of the cavity field, the membrane, and the dipoles on the 3–1 and 2–1 transitions, respectively, and $g_N = g\sqrt{N}$ is the atomic collective coupling strength. The cavity driving is given by the nonzero $\langle a_{in} \rangle$; the other Langevin noise terms have the following relevant correlations: $\langle c_3^{in}(t)c_3^{in\dagger}(t') \rangle = \gamma\delta(t-t')$, $\langle c_2^{in}(t)c_2^{in\dagger}(t') \rangle = \gamma_c\delta(t-t')$, $\langle a_{in}(t)a_{in}^\dagger(t') \rangle = \kappa\delta(t-t')$, $\langle b_{in}(t)b_{in}^\dagger(t') \rangle = \gamma_m(n_i + 1)\delta(t-t')$, and $\langle b_{in,\uparrow}(t)b_{in,\uparrow}(t') \rangle = \gamma_m n_i \delta(t-t')$. The initial occupancy of the mechanical resonator imposed by the external thermal reservoir T is denoted here by n_i .

Dressed cavity field response. In the steady state, we have $\langle a \rangle = \langle a_{in} \rangle / (\kappa + i\Delta_c - i\chi_{\text{EIT}})$ where $\Delta_c = \Delta_{\text{cav}} - 2G^2/\omega_m$, with $G = G_0\alpha$ ($\alpha = |a\rangle$). The EIT medium susceptibility is $\chi_{\text{EIT}} = ig_N^2 / [\gamma + i\Delta + \Omega^2/(\gamma_c + i\delta)]$. For a strongly absorbing medium ($g_N > \kappa, \gamma$), the cavity will be transparent only in a narrow frequency range around the two-photon (EIT) resonance. This emulates a cavity substantially narrower than its natural linewidth 2κ . Under the assumptions $\Omega^2 \gg \gamma_c\gamma$ and $\Omega \gg \gamma_c$ the cavity transmission spectrum becomes a Lorentzian peak centered around $\delta = 0$ with a modified half-width

$$\kappa_{\text{EIT}} \simeq \gamma_c + \kappa \frac{\Omega^2}{g_N^2}. \quad (2)$$

An effective sharpening of the cavity response around the two-photon atomic resonance can thus be obtained if narrow atomic resonances ($\gamma_c \ll \kappa$) and strong atom-cavity coupling strengths ($g_N \gg \Omega$) are used [6,7]. This tailoring effect can be used to engineer the coupling between the atoms and the membrane motion. For a simple physical understanding, one can Fourier analyze Eq. (1c) to derive the cavity response in the frequency domain in the presence of atoms. One sees in Fig. 1(c) the EIT sharpening of the cavity profile around the blue sideband, leading to the inhibition of the red sideband, which in turn improves cooling as compared to the situation where no atoms are present. Equations (1a)–(1d) can be linearized around their steady-state mean values, and the covariance matrix (CM) of the quantum fluctuations of all observables can be calculated numerically [14]. The most interesting physical situations correspond to tuning the dressed cavity field resonances to either the anti-Stokes or the Stokes motional sidebands. Here, the analysis is most conveniently performed by moving to the corresponding rotating frames.

Anti-Stokes sideband resonance: Cooling and state mapping. We first assume that the cavity and the atomic two-photon detunings are matched to the anti-Stokes motional frequency, $\delta = \Delta_c = \omega_m$. In the frame rotating at ω_m and neglecting off-resonant interactions, the equations for the fluctuations read

$$\dot{\tilde{c}}_3 = -\gamma\tilde{c}_3 + ig_N \tilde{a} + i\Omega\tilde{c}_2 + \tilde{c}_3^{in}, \quad (3a)$$

$$\dot{\tilde{c}}_2 = -\gamma_c\tilde{c}_2 + i\Omega\tilde{c}_3 + \tilde{c}_2^{in}, \quad (3b)$$

$$\dot{\tilde{a}} = -\kappa\tilde{a} + ig_N\tilde{c}_3 + iG\tilde{b} + \tilde{a}_{in}, \quad (3c)$$

$$\dot{\tilde{b}} = -(\gamma_m/2)\tilde{b} + iG\tilde{a} + \tilde{b}_{in}. \quad (3d)$$

where $\tilde{o} = oe^{-i\omega_m t}$. We look at the effective interaction between \tilde{c}_2 and \tilde{b} in the regime when $\gamma, \kappa \gg \gamma_c, \gamma_m, \omega_m$, that is, such that \tilde{c}_3 and \tilde{a} are the fast variables that can be adiabatically eliminated. We first identify the optical cooling rate $\Gamma_O = G^2/\kappa$, and the excited ground state decay rate $\Gamma_E = \Omega^2/\gamma$, with corresponding normalized rates $\gamma_O = \Gamma_O/(1+C)$ and $\gamma_E = \Gamma_E/(1+C)$, where $C = g_N^2/\kappa\gamma$ is the cooperativity parameter. We can now write for the reduced bipartite system

$$\dot{\tilde{c}}_2 = -(\gamma_c + \gamma_E)\tilde{c}_2 - i\sqrt{C\gamma_E\gamma_O}\tilde{b} + \tilde{c}_2^{in}, \quad (4a)$$

$$\dot{\tilde{b}} = -(\gamma_m/2 + \gamma_O)\tilde{b} - i\sqrt{C\gamma_E\gamma_O}\tilde{c}_2 + \tilde{b}_{in}, \quad (4b)$$

which show the renormalized bare effective decay rates of the system $\gamma_c + \gamma_E$ and $\gamma_m/2 + \gamma_O$ together with the coupling rate $\sqrt{C\gamma_E\gamma_O}$. The effective Langevin noise terms are expressed as $\tilde{c}_2^{in} = -i\sqrt{\gamma_E/(1+C)}c_3^{in}/\sqrt{\gamma} - \sqrt{\gamma_EC/(1+C)}a_{in}/\sqrt{\kappa} + c_2^{in}$, $\tilde{b}_{in} = i\sqrt{\gamma_O/(1+C)}a_{in}/\sqrt{\kappa} - \sqrt{\gamma_OC/(1+C)}c_3^{in}/\sqrt{\gamma} + b_{in}$. One can deduce an effective Hamiltonian, $H_{AS} \simeq \sqrt{C\gamma_E\gamma_O}(\tilde{b}^\dagger\tilde{c}_2 + \tilde{b}\tilde{c}_2^\dagger)$, that takes the form of the beam-splitter-like interaction extensively used in quantum optics and quantum information. We identify two regimes: (i) a cooling regime for $\gamma_O \ll \gamma_E$ and (ii) a state transfer (strong coupling) regime, for $\sqrt{C\gamma_E\gamma_O} \gg \gamma_E, \gamma_O, \gamma_c, \gamma_m n_i$, which we analyze analytically and numerically in the following.

When $\kappa_{\text{EIT}} \gg \gamma_c, \Gamma_O$ one can treat the atom-cavity subsystem as an effective bath for the mechanical degree of freedom [15]. The sharpening of the cavity response (EIT window) can inhibit Stokes scattering, leading to resolved sideband cooling. Assuming a bad cavity $\kappa \gg \omega_m$ (for which direct cavity-induced optomechanical cooling cannot reach the ground state), we first assume that $\kappa_{\text{EIT}} \ll \omega_m$ to resolve sidebands. Under these conditions, the effective cooling rate of the membrane can be shown to be $\Gamma = \Gamma_O/[1 + (\kappa_{\text{EIT}}/2\omega_m)^2]$, and the final mechanical occupancy is equal to

$$n_f \simeq \frac{\gamma_m}{\gamma_m + \Gamma} n_i + \frac{\Gamma}{\gamma_m + \Gamma} \left[\left(\frac{\kappa_{\text{EIT}}}{2\omega_m} \right)^2 + \frac{\gamma_c}{2\kappa_{\text{EIT}}} \right], \quad (5)$$

which is reminiscent of the resolved sideband optomechanical cooling limit [15], with κ being replaced by the sharper κ_{EIT} , but with an additional atomic noise reflected by the small term $\gamma_c/2\kappa_{\text{EIT}}$. Ground-state cooling then becomes possible for sufficiently strong optomechanical coupling and narrow cavity EIT resonances [7].

In the regime where $\sqrt{C\gamma_E\gamma_O}$ becomes larger than the effective decay, rates a coherent state transfer regime emerges. The conditions can be summarized by the following double inequality:

$$\frac{\kappa}{g_N} \ll \frac{G}{\Omega} \ll \frac{g_N}{\gamma}. \quad (6)$$

To illustrate the cooling and state transfer regimes more clearly, we now focus on a numerical example. We take a membrane with $\omega_m = (2\pi)200$ kHz, mechanical quality factor $Q_m \sim 10^7$, and effective mass 1 ng [11]; the thermal environment

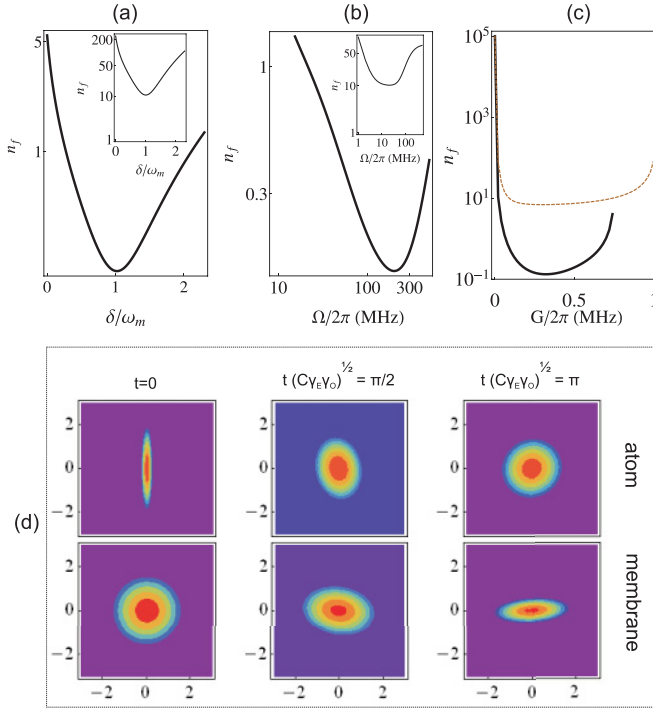


FIG. 2. (Color online) Cavity EIT cooling: (a) Logarithmic plot (of base 10) of n_f as a function of normalized two-photon detuning δ/ω_m . (b) Variation of n_f with Ω for $\delta = \omega_m$. (c) Variation of n_f with G for standard self-cooling with no atoms ($\Delta_c = \kappa/2$, dashed line) and cavity EIT cooling [$\delta = \omega_m$, $\Omega = (2\pi)300$ MHz, solid line]. The insets show the case of $N = 10^6$ atoms (see text). State mapping: (d) Time evolution of Wigner functions for an initially squeezed ground-state atomic spin. See text for parameters.

is at 1 K, with initial occupancy $n_i = 10^5$ at ω_m . For a 1-cm-long cavity with $\kappa = (2\pi)1$ MHz, one gets a single-photon optomechanical strength of the order $G_0 \simeq (2\pi)200$ Hz. To be in the EIT-resolved sideband regime $\kappa_{\text{EIT}} \ll \kappa$, one needs that $g\alpha \ll \Omega \ll g_N$, which implies $\alpha^2 \ll N$. Since the cooling rate scales with the number of photons, it is advantageous to use a large ensemble. For a $N = 10^8$ cold Rb cloud, obtained, for example, using three-dimensional (3D) molasses, with $\gamma = (2\pi)3$ MHz, $g = (2\pi)100$ kHz, and $\gamma_c \sim (2\pi)1$ kHz, and taking $\alpha \sim 10^3$ and $\Omega = (2\pi)300$ MHz, one gets $\kappa_{\text{EIT}} \simeq \kappa/10$ and $G \simeq (2\pi)200$ kHz. For these parameters, we numerically calculate the CM from Eqs. (1a)–(1d) and show in Fig. 2(a) the expected optimization of cooling when $\delta = \omega_m$. The effective cavity window then completely includes the anti-Stokes sideband for efficient cooling, $\kappa_{\text{EIT}} \gg \Gamma_0 = (2\pi)40$ kHz. Fixing $\delta = \omega_m$, Fig. 2(b) shows the variation of n_f with Ω . As expected from Eq. (5), the occupancy decreases as κ_{EIT} increases until the EIT window becomes too large to resolve the sidebands. The insets in Figs. 2(a) and 2(b) show the case of a smaller $N = 10^6$ cloud, for example, BEC, with $\alpha = 10^2$, $\Omega = (2\pi)30$ MHz, and $G \simeq (2\pi)20$ kHz, for which substantial cooling can still be observed. Similar results could also be achieved with ensembles with lower N , such as ion crystals [7,13], but would require higher bare optomechanical coupling strengths. We show in Fig. 2(c) a comparison between cavity EIT cooling and standard optimized cavity cooling (when no

atoms are present) with fixed $\Delta_c \simeq \kappa/2$ as a function of G . The obtainable temperature is about two orders of magnitude lower in the EIT cooling case while the cooling rate is enhanced by a factor of $\sim \kappa/\omega_m$.

We then check the validity of our RWA treatment indication of a strong coupling regime by taking the example of a reversible state mapping of a squeezed state. Starting with the atoms in a squeezed state with squeezing parameter $r = 1$ (such that the squeezed quadrature variance is reduced from $1/2$ to $e^{-2r}/2$) and the membrane in an initial thermal state with average phonon number 2, we numerically integrate Eqs. (1a)–(1d) and calculate the time evolution of the atom and membrane Wigner functions. To satisfy Eq. (6), we take $\Omega = (2\pi)100$ MHz and $G = (2\pi)500$ kHz. The ratios of the coupling strength $\sqrt{C\gamma_E\gamma_O}$ to the various decoherence rates ($\gamma_m n_i, \gamma_O, \gamma_E$) for the chosen illustration are $(12.5, 6.610^4, 5)$, and the state swapping at time $\pi/\sqrt{C\gamma_E\gamma_O}$ can be seen in Fig. 2(d). Notice that with $\alpha \simeq 250$ one needs $G_0 \sim (2\pi)2$ kHz, a value somewhat higher than that achieved with state-of-the-art SiN membranes [11].

Stokes sideband resonance: Atom-membrane entanglement. We now turn to the case where the cavity and the EIT medium are tuned to the Stokes sideband. Assuming $\delta = \Delta_c = -\omega_m$ and neglecting again off-resonant interactions, one gets a set of equations similar to Eqs. (1), with \tilde{b} being replaced by \tilde{b}^\dagger . Eliminating the fast variables in the frame rotating at $-\omega_m$, one can again deduce an effective Hamiltonian for the reduced atom-membrane system, which now takes the form of a parametric down-conversion process $H_S \simeq \sqrt{C\gamma_E\gamma_O}(\tilde{b}^\dagger \tilde{c}_2^\dagger + \tilde{b}\tilde{c}_2)$, known to generate bipartite entanglement from an initial bimodal separable state [10]. To quantify this entanglement, we calculate the logarithmic negativity E_N [16] (a computable measure for any mixed state of a bipartite system) by numerically integrating Eqs. (1a)–(1d) and looking at the steady state.

A closer look into the RWA equations of motion shows that despite the fact that the down-conversion process does lead to an entangled steady state, the assumption of $\Delta_c = -\omega_m$ strongly limits the achievable entanglement, owing to the occurrence of a parametric instability even for very small values of G . To get around the limitation imposed

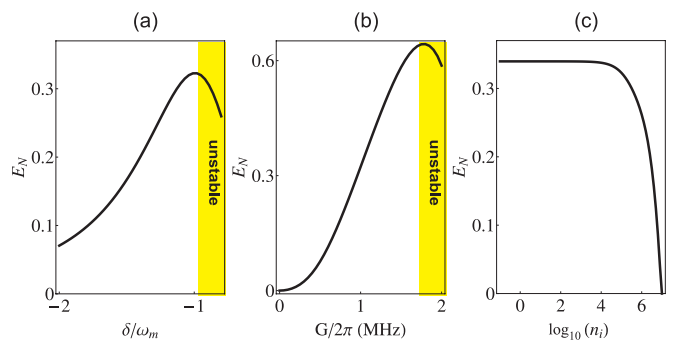


FIG. 3. (Color online) Atom-membrane steady-state entanglement: (a) Logarithmic negativity E_N as a function of δ for the parameters given in the text. (b) Variation of E_N with G for $\delta = -\omega_m$. (c) Variation of E_N with n_i , showing robustness of entanglement with respect to temperature.

by the parametric heating of the membrane, one can use a far-detuned cavity such that $|\Delta_c| \gg \kappa, \omega_m$. In such a case, higher values of G are allowed before the onset of parametric instability and considerable entanglement can in principle be generated, as illustrated in Fig. 3. As an example, we consider the parameters used for Fig. 2, except for $N = 10^4$ and $\Omega = (2\pi)1.2$ MHz, and choose $\Delta_c = -12\kappa$. The expected entanglement optimization at $\delta \simeq -\omega_m$ and increase with G are shown in Figs. 3(a) and 3(b). Under the condition $\delta \simeq -\omega_m$ and for $G = (2\pi)1$ MHz, Fig. 3(c) shows robustness with respect to T as E_N reaches 0 only at occupancies corresponding to ~ 20 K. Analytically, one can estimate in this regime that the effective atom-membrane coupling is $\Omega g_N G / \sqrt{g_N^4 + \gamma^2 \Delta_c^2}$ and that equating this to the thermal decoherence rate implies a vanishing E_N for $n_i \simeq 6 \times 10^6$, in agreement with Fig. 3(c). Detection of this entanglement could be performed by using two auxiliary light modes, one onto which the atomic state can be mapped and a second weakly probing the optomechanical response of the membrane [17].

Quantum state homodyne tomography of these modes could then be performed to reproduce the intracavity entanglement provided that this entanglement is strong enough to survive the detection back-action.

Conclusion and outlook. We have shown that a hybrid optomechanical approach in dealing with quantum effects at the mesoscale range defined by a mechanical resonator can be employed to enter regimes otherwise inaccessible in the bare optomechanical system. Strong coupling and entanglement in the unresolved sideband regime of a cavity-membrane system, for instance, can be engineered via the controllable atom-field EIT effect. Such a hybrid interface could provide a route for efficient readout, for example, and even long-distance quantum teleportation of a mechanical resonator quantum state.

Acknowledgments. M.D. and A.D. acknowledge support from the ESF Euroquam ‘‘CMMC’’ and EU ‘‘PICC’’ and ‘‘CCQED’’ projects. C.G. and H.R. acknowledge support from the NanoSci-E+ Project ‘‘NOIs.’’

-
- [1] T. J. Kippenberg and K. J. Vahala, *Science* **321**, 1172 (2008); I. Favero and K. Karrai, *Nature Photon.* **3**, 201 (2009); M. Aspelmeyer *et al.*, *J. Opt. Soc. Am. B* **27**, A189 (2010).
- [2] K. W. Murch *et al.*, *Nature Phys.* **4**, 561 (2008); F. Brenneke *et al.*, *Science* **322**, 235 (2008); T. P. Purdy *et al.*, *Phys. Rev. Lett.* **105**, 133602 (2010); M. H. Schleier-Smith *et al.*, e-print arXiv:1104.4623v1.
- [3] L. Tian and P. Zoller, *Phys. Rev. Lett.* **93**, 266403 (2004); P. Treutlein, D. Hunger, S. Camerer, T. W. Hansch, and J. Reichel, *ibid.* **99**, 140403 (2007); C. Genes, D. Vitali, and P. Tombesi, *Phys. Rev. A* **77**, 050307(R) (2008); K. Hammerer, M. Aspelmeyer, E. S. Polzik, and P. Zoller, *Phys. Rev. Lett.* **102**, 020501 (2009); K. Hammerer *et al.*, *ibid.* **103**, 063005 (2009); S. Singh, M. Bhattacharya, C. Dutta, and P. Meystre, *ibid.* **101**, 263603 (2008); N. Lambert *et al.*, *ibid.* **100**, 136802 (2008); P. Rabl *et al.*, *Phys. Rev. B* **79**, 041302(R) (2009).
- [4] C. Genes, H. Ritsch, and D. Vitali, *Phys. Rev. A* **80**, 061803 (2009).
- [5] K. Hammerer *et al.*, *Phys. Rev. A* **82**, 021803 (2010); D. Hunger *et al.*, e-print arxiv:1103.1820.
- [6] M. D. Lukin *et al.*, *Opt. Lett.* **23**, 295 (1998); G. Hernandez, J. Zhang, and Y. Zhu, *Phys. Rev. A* **76**, 053814 (2007); H. Wu, J. Gea-Banacloche, and M. Xiao, *Phys. Rev. Lett.* **100**, 173602 (2008).
- [7] M. Albert, A. Dantan, and M. Drewsen, *Nature Photon.* **5**, 633 (2011).
- [8] F. Elste, S. M. Girvin, and A. A. Clerk, *Phys. Rev. Lett.* **102**, 207209 (2009).
- [9] G. Morigi, J. Eschner, and C. H. Keitel, *Phys. Rev. Lett.* **85**, 4458 (2000).
- [10] M. A. Nielsen and I. L. Chuang, *Quantum Computation and Quantum Information* (Cambridge, Cambridge University Press, 2000).
- [11] J. D. Thompson *et al.*, *Nature (London)* **452**, 72 (2008); D. J. Wilson, C. A. Regal, S. B. Papp, and H. J. Kimble, *Phys. Rev. Lett.* **103**, 207204 (2009); J. C. Sankey *et al.*, *Nat. Phys.* **6**, 707 (2010).
- [12] A. T. Black, H. W. Chan, and V. Vuletic, *Phys. Rev. Lett.* **91**, 203001 (2003); Y. Colombe *et al.*, *Nature (London)* **450**, 272 (2007).
- [13] P. Herskind *et al.*, *Nat. Phys.* **5**, 494 (2009).
- [14] C. W. Gardiner and P. Zoller, *Quantum Noise* (Springer-Verlag, Berlin, 2000).
- [15] I. Wilson-Rae, N. Nooshi, W. Zwerger, and T. J. Kippenberg, *Phys. Rev. Lett.* **99**, 093901 (2007); F. Marquardt, J. P. Chen, A. A. Clerk, and S. M. Girvin, *ibid.* **99**, 093902 (2007); A. Dantan, C. Genes, D. Vitali, and M. Pinard, *Phys. Rev. A* **77**, 011804(R) (2008); C. Genes, D. Vitali, P. Tombesi, S. Gigan, and M. Aspelmeyer, *ibid.* **77**, 033804 (2008).
- [16] J. Eisert, Ph.D. thesis, University of Potsdam, 2001; G. Vidal and R. F. Werner, *Phys. Rev. A* **65**, 032314 (2002).
- [17] D. Vitali *et al.*, *Phys. Rev. Lett.* **98**, 030405 (2007).